ISSN 8755-6839

SCIENCE OF **TSUNAMI HAZARDS**

Journal of Tsunami Society International

Volume 41 **Number 4** **2022**

NUMERICAL MODELING OF A TSUNAMI OF LANDSLIDE ORIGIN IN THE KURIL BASIN

R.Kh. Mazova, A.A. Kurkin, D.A. Okunev

Nizhny Novgorod State Technical University n.a. R.E. Alekseev, Nizhny Novgorod, Russia. e-mail: raissamazova@yandex.ru

The work is devoted to the study of landslide-induced tsunami in the area of the Sea of Okhotsk on the western slope of the Kuril Basin. Landslide areas, up to 2 km in size, are located on the North Hokkaido marginal plateau and near the Patience Ridge. Possible strong tsunamis generated by landslide processes in the Kuril depression, which represent a potential hazard for the eastern coast of the island, are considered. Sakhalin Island, where there is currently an intensive development of infrastructure related to the development of oil and gas fields. To assess the risks, it is necessary to carry out numerical simulation of possible catastrophic landslide processes in the Kuril Basin and tsunamis generated by these processes. In this work, such modeling was carried out on the basis of a solid-block segmental model of a landslide body.

***Key words**: Sea of Okhotsk, Kuril basin, landslide slope, solid block segmental model of landslide body, numerical modeling.*

1. INTRODUCTION

The tsunami problem is especially relevant for the Russian Far East. There are many studies on the tsunami hazard of the Sea of Okhotsk and the Kuril-Kamchatka region, both for seismic events and for landslides (see, for example, [1-7]). The waves formed by landslides often have a shorter period and length compared to the waves that appeared as a result of an earthquake, and diminish rather quickly. However, their destructive power is comparative with that of seismic tsunami. Large waves caused by landslides have been observed quite often in recent decades. So, for example, on June 17, 2017, a landslide descended into the Karrats Fjord (Greenland), which caused a tsunami more than 90 meters high, although the magnitude of the earthquake was M ~ 4 [8]. A well-known tsunamigenic underwater landslide Storegga along the continental slope on the coast of Norway, which was about 290 km wide and extended for more than 800 km. The maximum height of tsunami waves reached 10–12 m, and in the Shetland Islands it exceeded 20 m [4]. On December 22, 2018, a tsunami occurred in the Sunda Strait, in the southwestern part of Indonesia, which was presumably caused by a landslide (from the slope of the Anak-Krakatau volcano) in an area of 64 hectares [9]. Widespread landslides were noted in the southern part of the eastern slope of Sakhalin Island (western slope of the Kuril basin) [3].

Under computation of tsunami waves caused by landslides, the main point is the choice of a model for describing the behavior of a landslide in numerical simulation. Currently, there are a number of models, the main of which are the model of solid block [10-13], and the model of a viscous or viscoelastic fluid [14-17], etc. In the model of solid block, the motion of a landslide is described within the framework of the rigid body dynamics, and for generation of surface water waves, shallow water equations are used. An underwater landslide is modeled by a rectangular block that moves with a constant speed on the bottom or sea slope. At the beginning of the landslide movement, in the general case, a dipole wave is generated — an elevation of water (crest) at the front edge of the landslide and a dip in the water level (trough) at its back. The relationship between landslide and water was based on the assumption of an impermeable solid bottom interacting with water for a certain period of time. A landslide usually consists of disconsolidated sediments that travel downslope and accumulate in a new location. The process of interaction of disconsolidated deposits does not always imply volume conservation.

In a number of cases, when landslide materials, such as lava, river sediments, or snow, behave approximately in the same way as a plastic Bingham fluid, an underwater plastic landslide is studied using the viscoelastic fluid approximation (see, for example, [14, 15]). In this model, the nonlinear equations of shallow water are used both for the movement of a landslide and for the generation of surface water waves. The variety of models of wave generation on the water surface by an underwater landslide leads to a difference in its parameters, which, of course, affects the characteristics of the waves generated on the coast (see, e.g., [13, 18-22]). Recently, several new models of landslide processes have been developed [23-25]. In contrast to these models, there is an elastic-plastic model of a landslide [26], which takes into account both the morphology of the landslide body and the mechanical characteristics of the sliding body components during the sliding process. At the same time, part of the sedimentary material is shifted from the upper part of the landslide body down the slope. When the elastic-plastic sedimentary layer slips, it generates a surface water wave, which is formed until the landslide stops, and then propagates over the water area [27, 28].

The complexity of the modeling problem is associated with the localization of an underwater landslide, as well as with its initial displacement. In addition, it is important how

complex the geometry of the underwater part of the slope along which the landslide moves is. During the underwater localization of a landslide, a long wave is formed on the surface of the water during the sliding process. As is known, at the beginning of a landslide movement, in the general case, a dipole wave is generated — an elevation of water (crest) at the front edge of the landslide and a dip in the water level (trough) at its back. As a result, the surface wave splits into two waves. The first train is moving towards the open sea, and the second one, consisting of two low waves and a crest, is moving towards the coastline.

As known, on Sakhalin Island, there are enterprises for the extraction and processing of oil, there are numerous settlements. With any significant earthquake or landslide process in the nearby zone, followed by a tsunami to the coast of Sakhalin Island, huge loss of human and material are possible. A wide distribution of landslides was noted in the southern part of the eastern slope of Sakhalin Island (western slope of the Kuril basin),

2. PROBLEM STATEMENT

This paper considers the landslide process on the western slope of the Kuril Basin. As noted in [3], the material was obtained in five marine expeditions in 2004-2015 during the survey of the Kuril basin. On the western slope of the Kuril basin, based on the data of bathymetric and seismic surveys, areas of possible landslide processes were identified. Using the data of these studies, the work considered the western slope of the Kuril Basin and the western part of the basin itself. The data of [3] made it possible to identify sections of the slope that may be subject to destruction. A map of landslide hazard from landslides in the Kuril Basin is shown in fig. 1. The red dots mark the localizations of the largest landslide slopes, the arrows indicate the landslide centers considered in [3].

In this paper, we consider the distribution of maximum tsunami wave heights along the eastern coast of Sakhalin Island, which, with possible landslide processes on the western slope of the Kuril Basin, will be most susceptible to such waves. To do this, the paper considers several options for the implementation of the landslide process in the Kuril basin. The shelf area is occupied by the South Sakhalin sedimentary basin, which consists of the Aniva and Patience troughs. A graphical illustration of the profiles of the main landslide slopes taken from [3] is shown in Fig. 2. Two hypothetical centers of landslides were chosen in the work, located under the numbers 1 and 4 presented in Fig. 2 [3]. The landslide movement is modeled as the movement of a rigid body, divided into a number of blocks-segments, and the landslide process was modeled by the dynamic vertical displacement of segment blocks along the landslide slope, simulating the sliding of the landslide mass. The kinematics of the movement of blocks is determined by the schematic behavior of the landslide movement, corresponding to a typical implementation of the calculation within the framework of the elastic-plastic model — sliding of the upper part of the landslide layer with a simultaneous increase in the thickness of the lower part of the slope (see, e.g., [28]). To implement this simulation, the landslide body is represented by 4 segmental blocks located along the slope. This process, can be roughly approximated by the displacement of the upper segment blocks first downwards, with the simultaneous displacement of the lower blocks upwards. To model various landslide processes for each scenario, their own options for shifting the blocks into which the landslide is divided are proposed. Data are presented for each option in Tables 1 and 2 (see below). In this case, the two upper blocks sequentially move down, with the simultaneous sequential movement of the two lower blocks upwards (see Tables below). Figure 3

shows the computational domain used for numerical simulation: 44.5° — 55°N (N), 141.7°-149°E (E). Since the computation of the tsunami hazard of the eastern part of Sakhalin is of particular importance, due to its population and the presence of dense infrastructure along the coasts, in the area of populated areas such as the cities of Poronaysk, Makarov, Dolinsk, Korsakov and Nogliki, virtual tide gauges were set up to record possible maximum wave heights on the calculated 5-meter isobath.

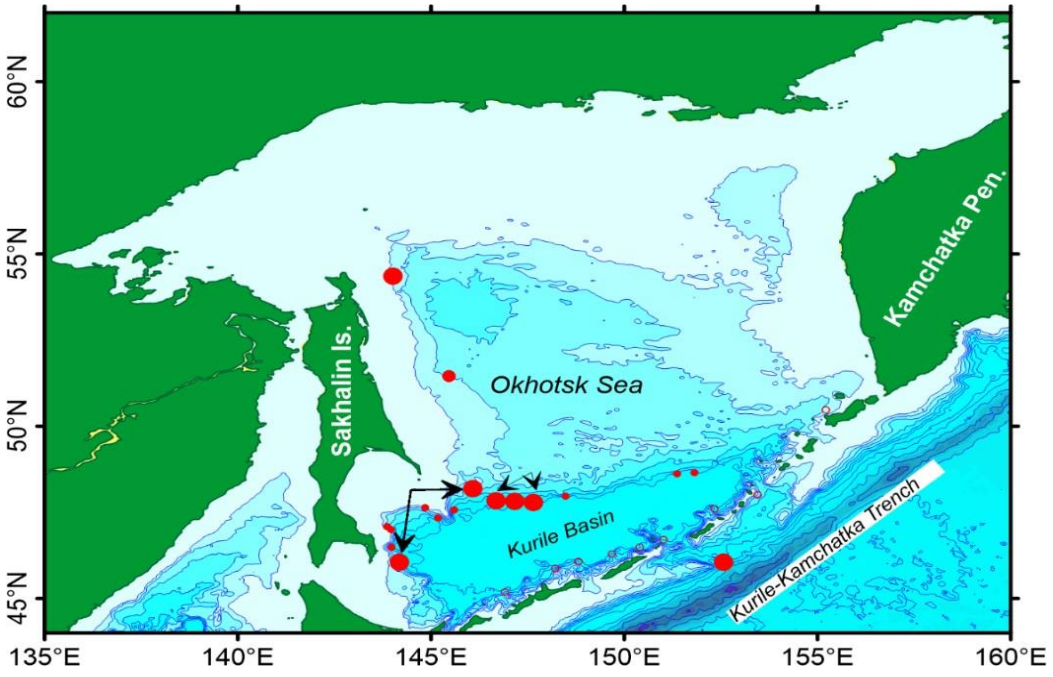

Fig. 1. Map of landslide hazard from landslides in the Kuril basin [3].

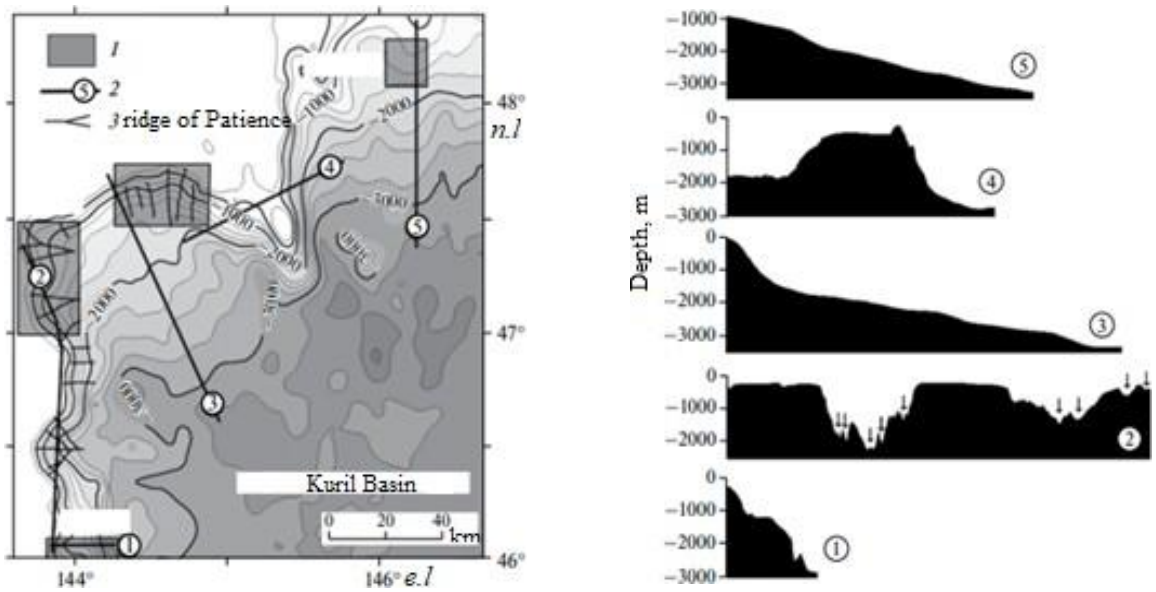

a) *b)*

Fig. 2. a) Bathymetric map of the study area. Circles with numbers indicate the areas of landslide localization; b) Bathymetric profiles illustrating landslide slopes in the study area [3].

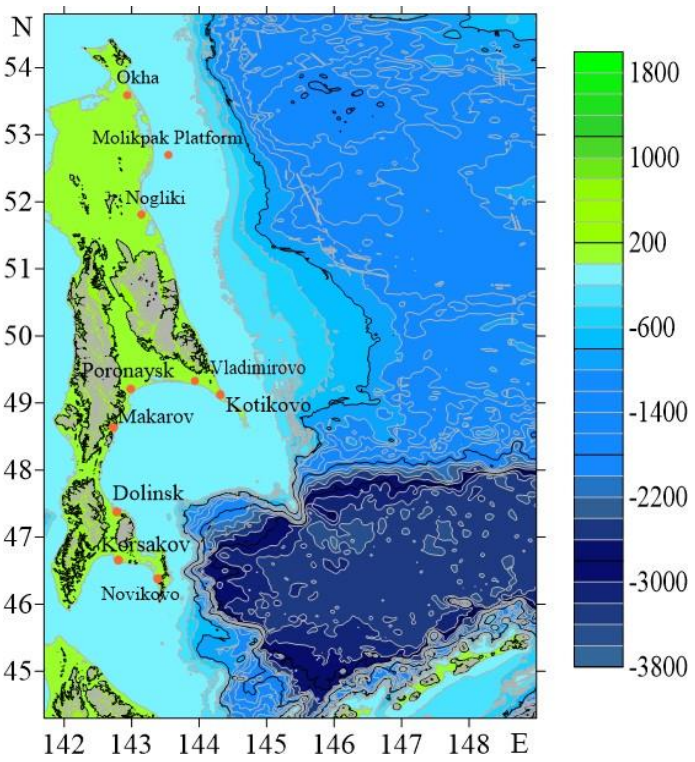

Fig. 3. Computed water area for modeling the landslide process in the Kuril basin

For a more detailed analysis of the generation of the tsunami source obtained during the movement of an underwater landslide, larger-scale areas of the water area shown in Fig.4 were considered. Fig. 4 shows the possible localization of landslide sources modeled by segment blocks for cases (1) and (4) depicted in Fig. 2b.

Thus, two landslide centers were considered in the Kuril depression: near the eastern part (Cape Patience) and near the southeastern part of Sakhalin Island (Cape Aniva). To simulate possible landslide processes, we will assume that the landslide precedes a virtual earthquake with a magnitude of M ~ 7.

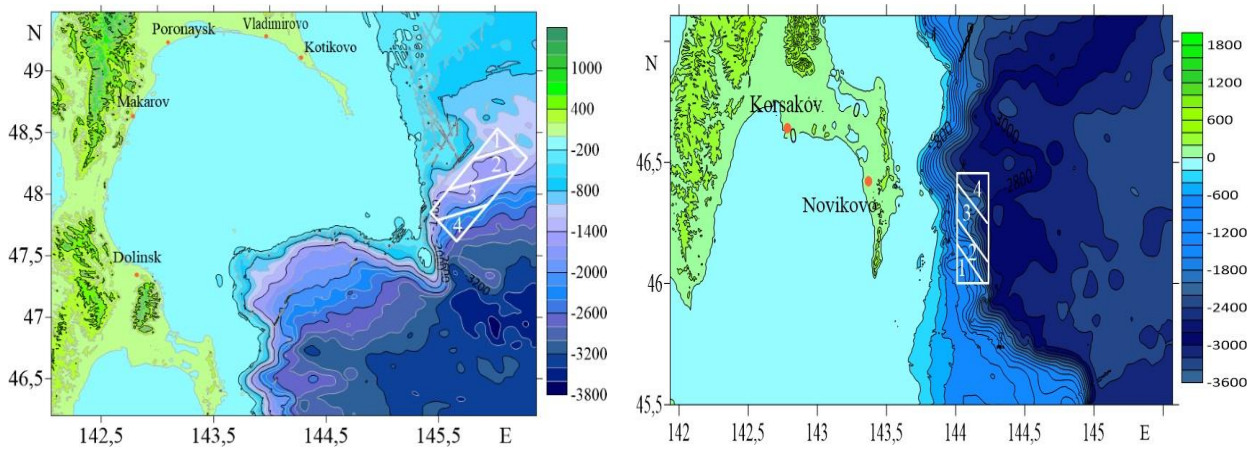

a) *b*)

Fig.4.a) Design water area for the first landslide (Scenario 1);

b) Estimated water area for the second landslide (Scenario 2).

3. MATHEMATICAL STATEMENT OF THE PROBLEM

To calculate the generation and propagation of long waves on the water surface caused by the movement of an underwater landslide, a system of nonlinear shallow water equations (1) is used. Numerical simulation was carried out using an upgraded software package based on a scheme with high algorithmic versatility proposed in [29]. To describe the generation and propagation of a wave caused by the movements of segmental solid blocks in the landslide source, a nonlinear system of shallow water equations in a two-dimensional formulation [27, 28, 30] was used

$$\begin{cases} \dfrac{\partial u}{\partial t}+u\dfrac{\partial u}{\partial x}+v\dfrac{\partial u}{\partial y}=-g\dfrac{\partial \eta}{\partial x} \\ \dfrac{\partial v}{\partial t}+u\dfrac{\partial v}{\partial x}+v\dfrac{\partial v}{\partial y}=-g\dfrac{\partial \eta}{\partial y} \\ \dfrac{\partial \eta}{\partial t}+\dfrac{\partial}{\partial x}[(\eta+H-B)\,u]+\dfrac{\partial}{\partial y}[(\eta+H-B)\,v]=\dfrac{\partial B}{\partial t} \end{cases} \quad (1)$$

where η is the displacement of the water surface, H is the depth of the basin, u and v are the components of the horizontal wave velocity. The evolution of the function B (x, y, t) in these equations was determined by the kinematic motion of the block segments. The beginning of the landslide movement, modeled by the movement of segmental blocks along the underwater slope. At the same time, it was assumed that there is a clear boundary between the liquid and the landslide body — the density of water is considered constant, the density of the landslide is also constant. At the last sea point at a depth of 5 m, the condition of total reflection is set (vertical a wall that makes it possible to fix the maximum and minimum values of the wave level shift at this depth.

3. Numerical modeling of a tsunami in the Sea of Okhotsk from a landslide source on the southwestern slope of the Kuril Basin.

3.1. Scenario 1.

Numerical simulation of a tsunami in the Sea of Okhotsk from a landslide source on the western slope of the Kuril Basin (Scenario 1). When considering Scenario 1, a hypothetical block-segment landslide source was modeled with a center at the point 48.27°N, 146.04°E [3]. The coordinates of the block segments, the displacement values of the blocks and their movement dynamics are given in Table 1.

Table 1. Kinematics of movement of segmental blocks in a landslide source (Scenario 1)

	Block 1	Block 2	Block 3	Block 4
x1	145.8212	145.5943	145.4266	145.4938
y1	48.2992	48.0435	47.8527	47.7859
x2	146.0229	145.8212	145.5943	145.9307
y2	48.5290	48.2992	48.0435	47.9098
x3	146.1558	146.1589	146.1793	145.6637
y3	48.4133	48.3805	48.1785	47.6203
x4	146.1589	146.1793	145.9307	145.6557
y4	48.3805	48.1785	47.9098	47.6203
Start time of movement (s)	0	20	30	40
Total time of movement (s)	30	20	30	30
Final time of movement (s)	30	40	60	70
Height (m)	-3	-2	2	3

The complete computational area with the localization of the landslide source for the implementation of Scenario 1 is shown in Fig. 5.

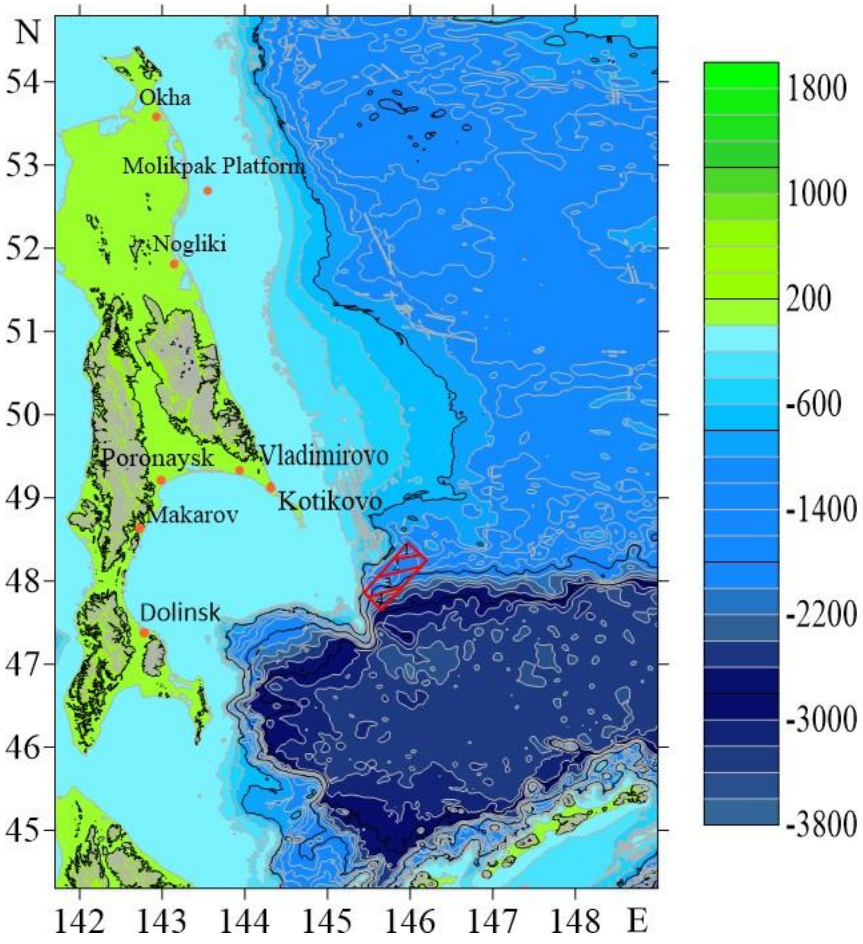

Fig. 5. Computed water area with the localization of the landslide source for Scenario 1

Figure 6 shows the results of numerical simulation of the generation of a tsunami source by a four-segment landslide source. It is clearly seen that when the first two segments move down the slope, the wave surface moves down (Fig. 6a, b), but simultaneously with this process, segments 3 and 4 rise, which corresponds to the upward displacement of the wave surface above these segments (Fig. 6b,c,d). Figure 6e,f shows the first moments of wave propagation from the tsunami source.

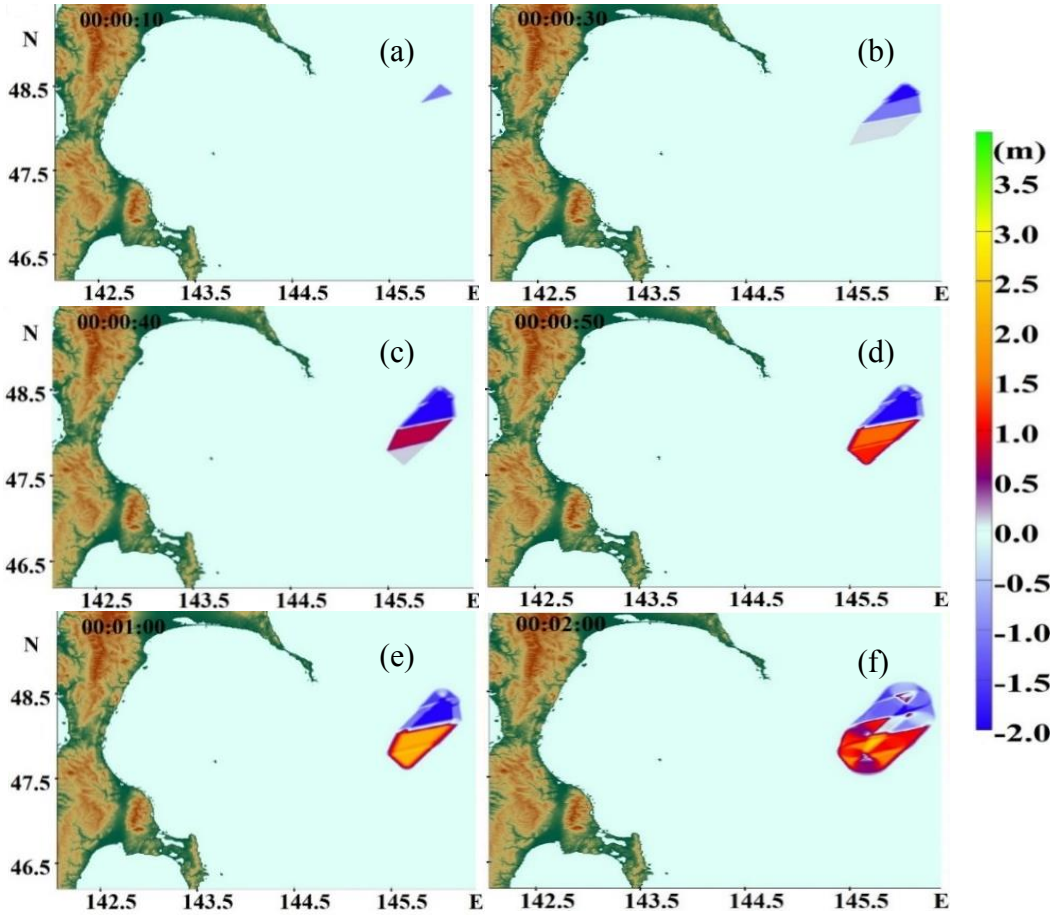

Fig. 6. Generation of a tsunami source in numerical simulation of a landslide process under Scenario 1

Figure 7 shows the further propagation of tsunami waves in a part of the Sea of Okhotsk (Fig. 7a-c) towards the Kuril Islands and Sakhalin Island. Displacement wave fields were obtained along Terpenya Bay and the eastern coast of Sakhalin Island. So, at t = 40 minutes (Fig. 8d), one can see how the wave front reached Cape Patience, Cape Aniva and began to spread in the Gulf of Patience. Figure f 7 shows how the wave moves towards the coast of the Gulf of Patience with a height ranging from 0.5 to 1.5 meters. Figure f 7 clearly shows how the wave front propagates along the east coast, towards the city of Okha. East

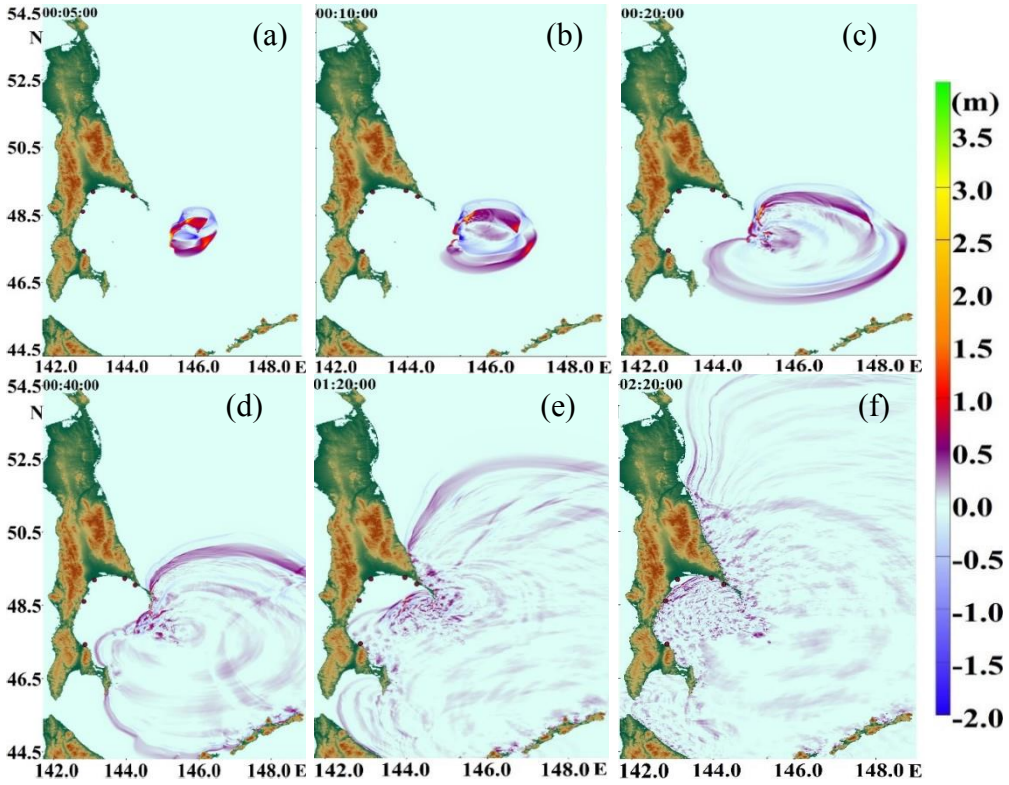

Fig. 7. Propagation of wave fronts in the Sea of Okhotsk (Scenario 1)

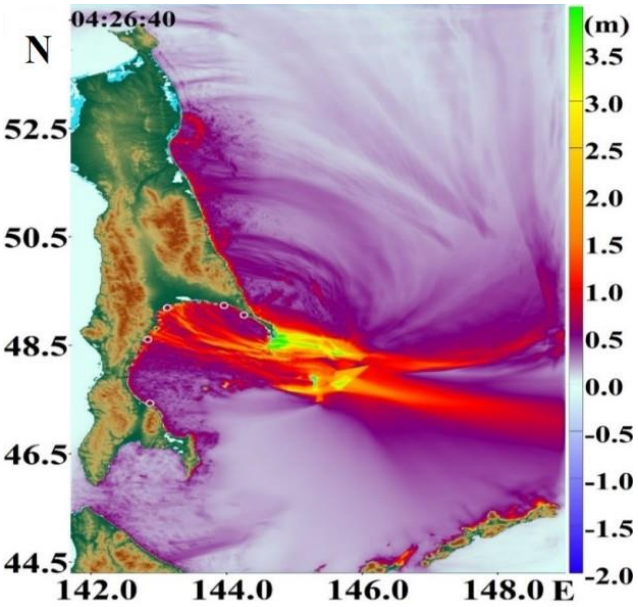

Fig. 8. Distribution of wave heights over the estimated water area during implementation Scenario 1

Figure 8 shows the distribution of heights over the computed water area under the implementation of Scenario 1 (Fig. 5). Almost along the entire coast, wave heights are observed in the range from 1-1.5 m. However, there are local areas with high heights, which is well observed in Fig. 9, which shows a 2D histogram of the distribution of maximum wave heights along the southeastern part of the coast of Sakhalin Island . It is clearly seen that the peak of heights falls on Cape Patience (144.8 E) and reaches 14 meters

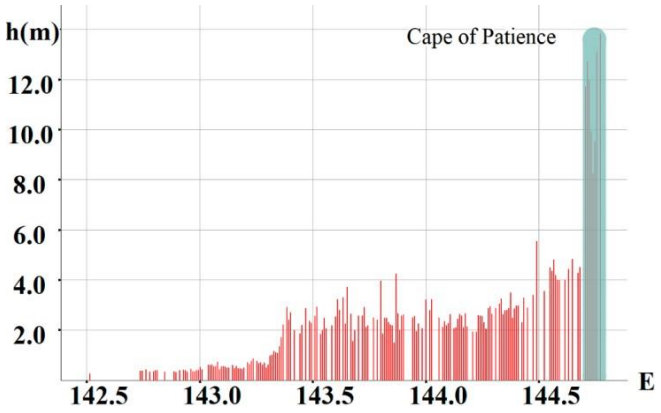

Fig. 9. Height Distribution Histogram (Scenario 1)

Figure 10 shows 3D histograms of the distribution of maximum wave heights along the eastern coast of Sakhalin Island on a 5-meter isobath. It can be seen that for this problem statement, the maximum wave heights reach 14 meters, while the average values do not exceed 1.5-3 meters.

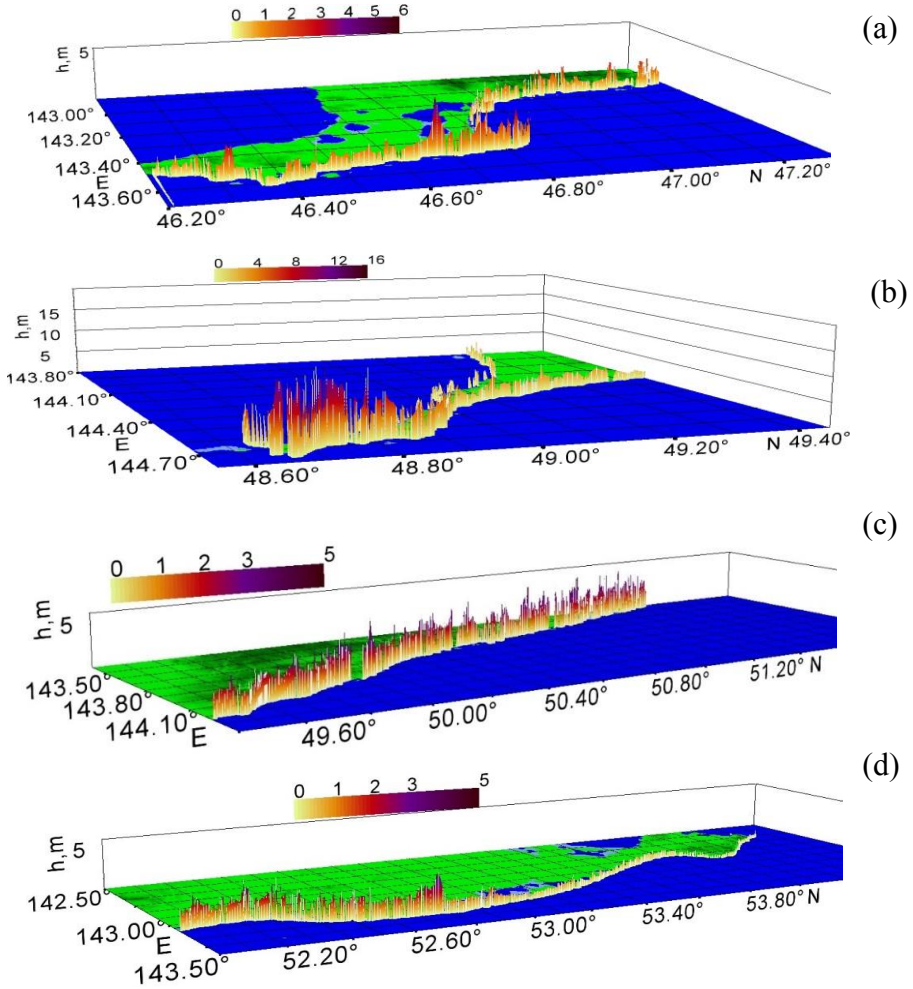

Fig. 10. 3D histograms of wave heights in some parts of the coast of about. Sakhalin under Scenario 1: a) coastal area near Cape Aniva and the cities of Dolinsk and Makarov; b) a section of the coast near the points of Kotikovo and Vladimirovo, as well as Cape Terpenya; c-d) sections of the northeastern coast of Sakhalin Island.

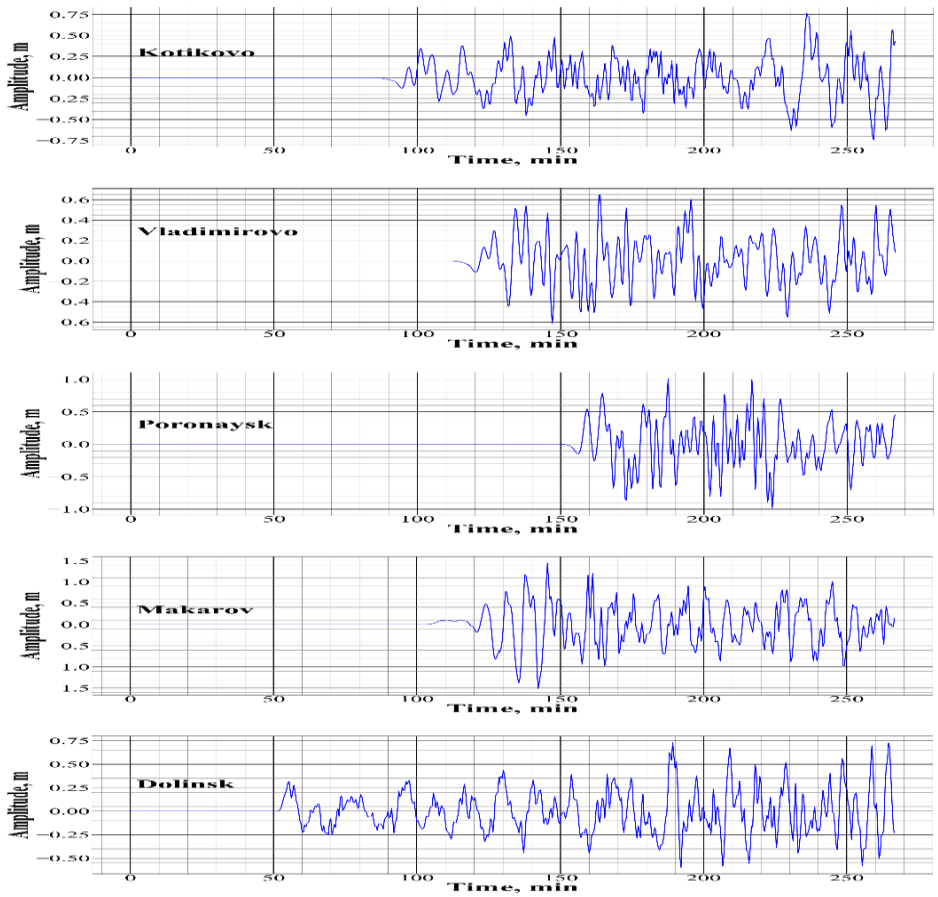

Fig. 11. The records from virtual tide gauges off the coast of Terpenya Bay (Sakhalin Island)

Figure 11 shows the data of records of virtual tide gauges set up in five points (Fig. 11, points 1-5). It is clearly seen on the tide-gauge records that the phase of the wave approach to the shore remains the same as in the first calculation at three points: Kotikovo, Vladimirovo and Poronaysk, the arrival of the first wave was accompanied by a slight rundown, where the vertical displacement was up to 0.2 m. At such points as Dolinsk and Makarov, the first wave was an elevation wave in the region from 0.25 to 0.5 m. You can also see that a train of waves approaches each point where virtual tide gauges are located, and the first positive wave nowhere was the maximum. The maximum wave height was recorded in the area of Makarov, when the fourth wave approached, with a height of more than 1 m. According to the tide-gauge records, the scatter of the maximum and minimum sea level heights is clearly visible, which is 2.96: from +1.45 to-1.51m.

3.2. Scenario 2.

To implement the Scenario 2, a hypothetical variant of a block-segment landslide source was modeled in the Kuril basin, near the Aniva cape, consisting of 4 segments (Fig. 12, see also Fig. 4 (b))]. The coordinates of the block segments, the displacement values of the blocks, and their dynamics of movement are given in Table 2. Figure 13 shows 6 times of generation of the tsunami source by the landslide source.

Thus, the formation of a tsunami source is clearly visible: at a) t = 10 sec, the downward movement of the first segment gives a decrease in the still water level by 3 m; b) t = 30 sec the second segment moves down by 2 m, and the third segment starts moving up by 2 m; c) t = 40 sec

the fourth segment begins to move, which gives a vertical displacement of the wave surface by 3 m. The time of formation of the tsunami source is 1 minute 10 seconds. Figure 13e shows the formed wave front at time $t = 2$ minutes.

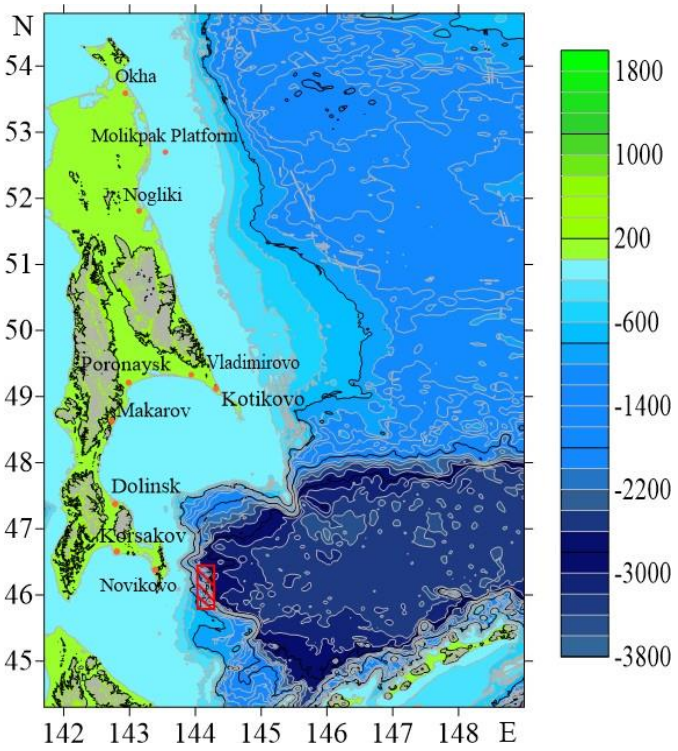

Fig. 12. Computation water area with the localization of the landslide source for Scenario 2

Table 2. Kinematics of movement of segmental blocks in a landslide Source (Scenario 2)

	Block 1	Block 2	Block 3	Block 4
x1	144.0324	144.0312	144.0111	144.0105
y1	45.7919	45.9696	46.1607	46.3472
x2	144.0312	144.0111	144.0105	144.0111
y2	45.9696	46.1607	46.3472	46.4092
x3	144.2567	144.2379	144.2377	144.2375
y3	45.7908	45.9398	46.1417	46.4079
x4	144.2157	144.2567	144.2379	144.2377
y4	45.7771	45.7908	45.9398	46.1417
Start time of movement (s)	0	20	30	40
Total time of movement (s)	30	20	30	30
Final time of movement (s)	30	40	60	70
Height (m)	-3	-2	2	3

Figure 14 shows the results of numerical simulation of tsunami wave propagation in a part of the Sea of Okhotsk. The wave from the source begins to propagate towards the Kuril Islands, Hokkaido Island and Sakhalin Island. Figure 14,b shows that when t = 10 min the wave reached Cape Aniva. Further, the wave front continued to propagate towards Aniva Bay and Cape Kostroma with wave heights in the range of 0.5 to 1.5 meters (Fig. 14c,d). At t = 1 hour 20 minutes (Fig. 14,f), the tsunami wave reached the entire coast of Aniva Bay. In Fig. 14,e, the wave propagates along the eastern coast of Sakhalin Island. As can be seen in Figure 15 and Figure 16, the average wave height is 1-2 meters, while Cape Aniva has a maximum wave height of 11.5 meters. It is clearly seen that some of the large waves reached Cape Kostroma. Figure 17 shows 3D histograms that confirm the conclusion about the average wave range of 1-2 meters, excluding Cape Aniva. Figures 17a and 17c show histograms of wave heights along Cape Aniva, where a wave peak is visible in the interval (46.2-46.4 N), the value of which reaches 12 meters. In Fig. 17d, in the range (142.4-142.8 E), the Korsakov and Novikovo points are located, where the average wave value does not exceed 1 meter. Also, in the range from (142 - 142.2 E) a tsunami wave comes to Cape Kostroma with a height of about 4-6 meters. The histogram in Fig. 17b shows the Gulf of Patience, where the average range of tsunami waves is 0.2 – 0.6 meters.

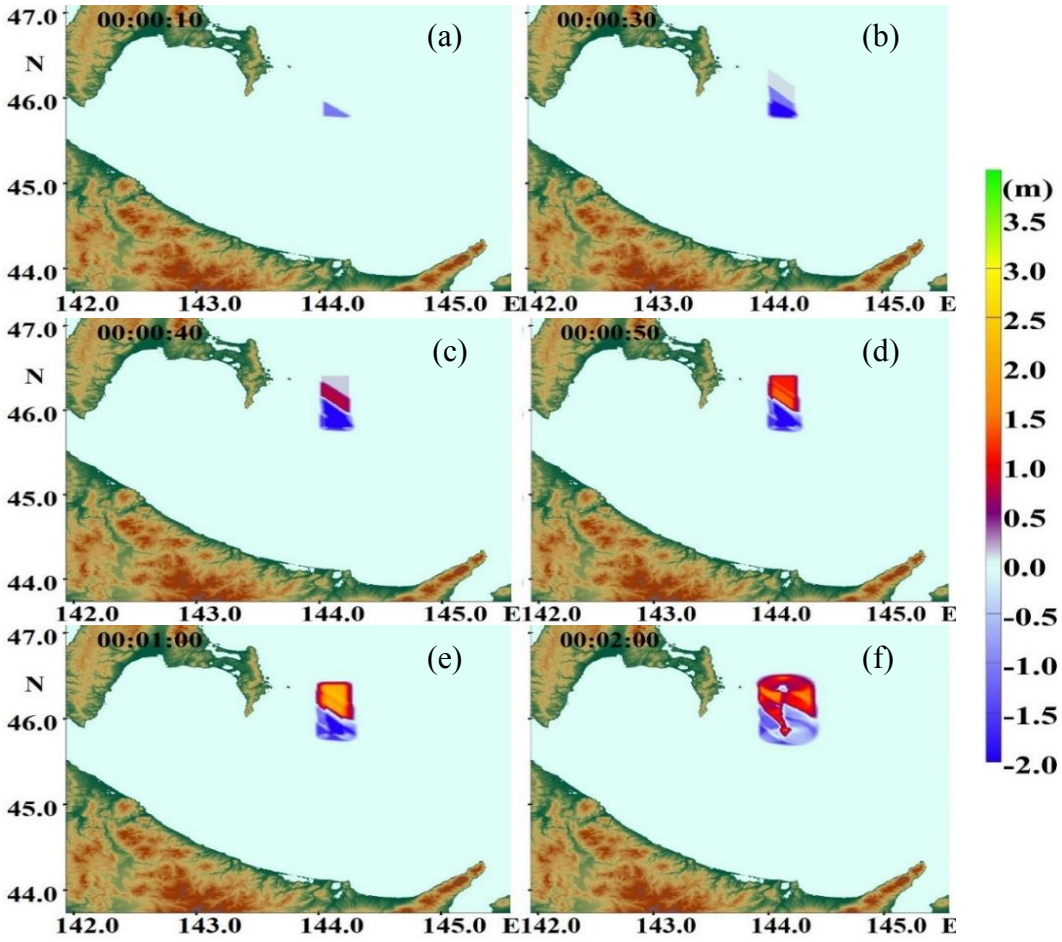

Fig.13. Generation of a tsunami source in numerical simulation of a landslide process under Scenario 2

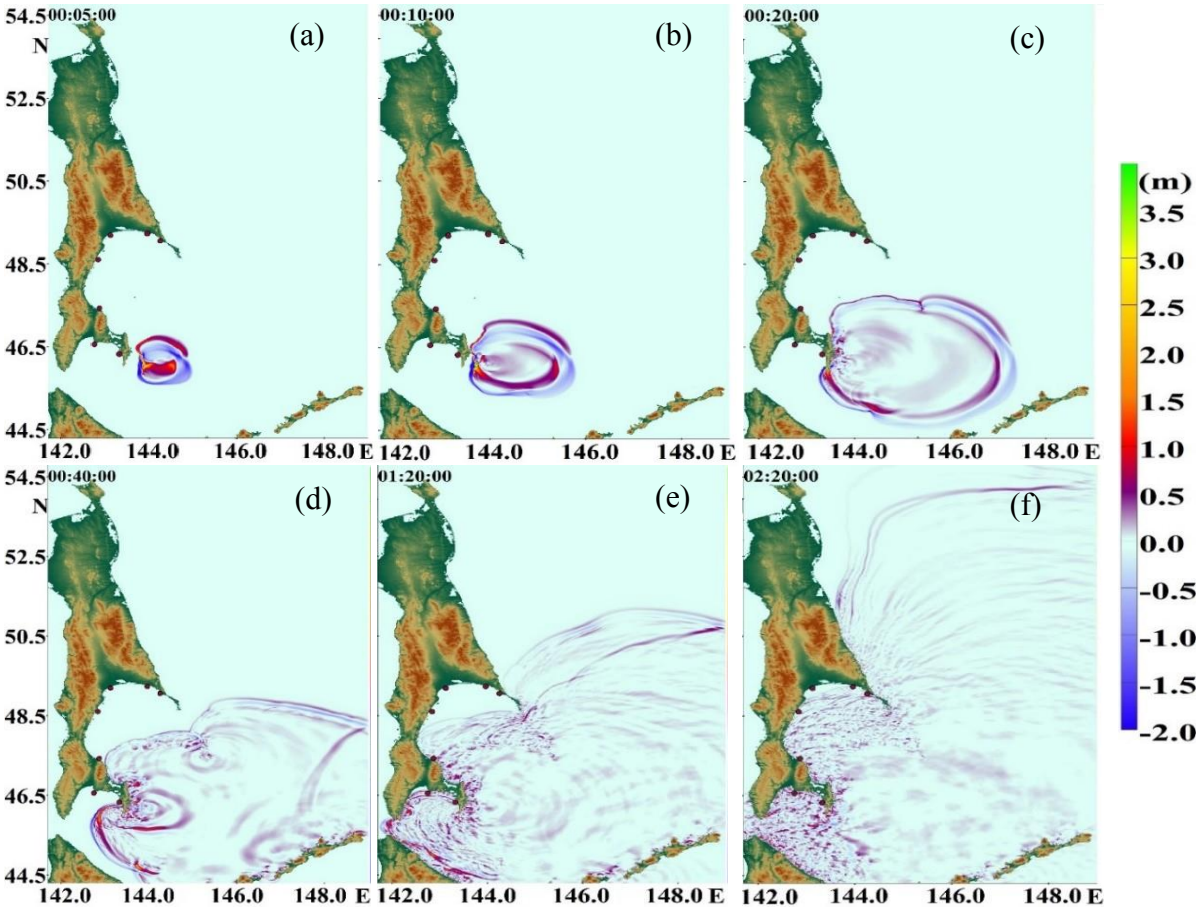

Fig.14. Propagation of wave fronts in the Sea of Okhotsk (Scenario 2)

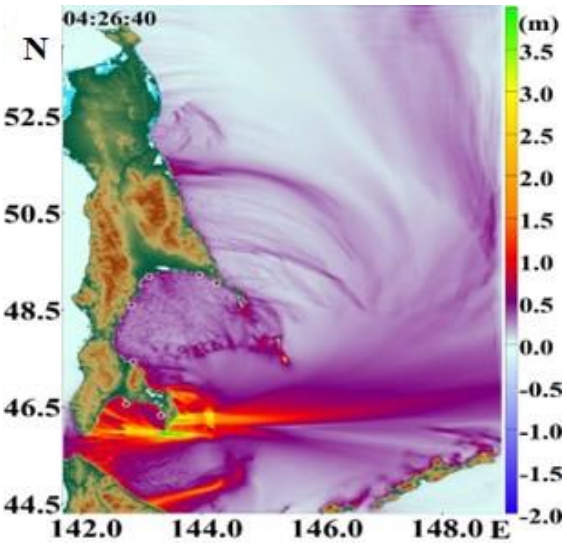

Fig. 15. Distribution of wave heights over the estimated water area during implementation Scenario 2

For a more detailed analysis of the computation, virtual tide gauges were set in points (1-7), the tide gauges from which are shown in Fig.18.

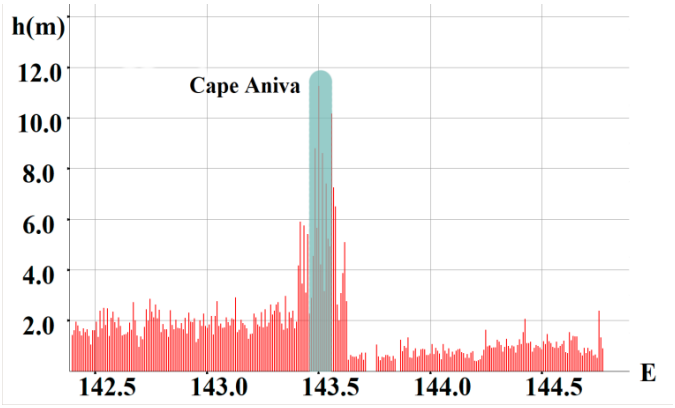

Fig.16. Height Distribution Histogram (Scenario 2)

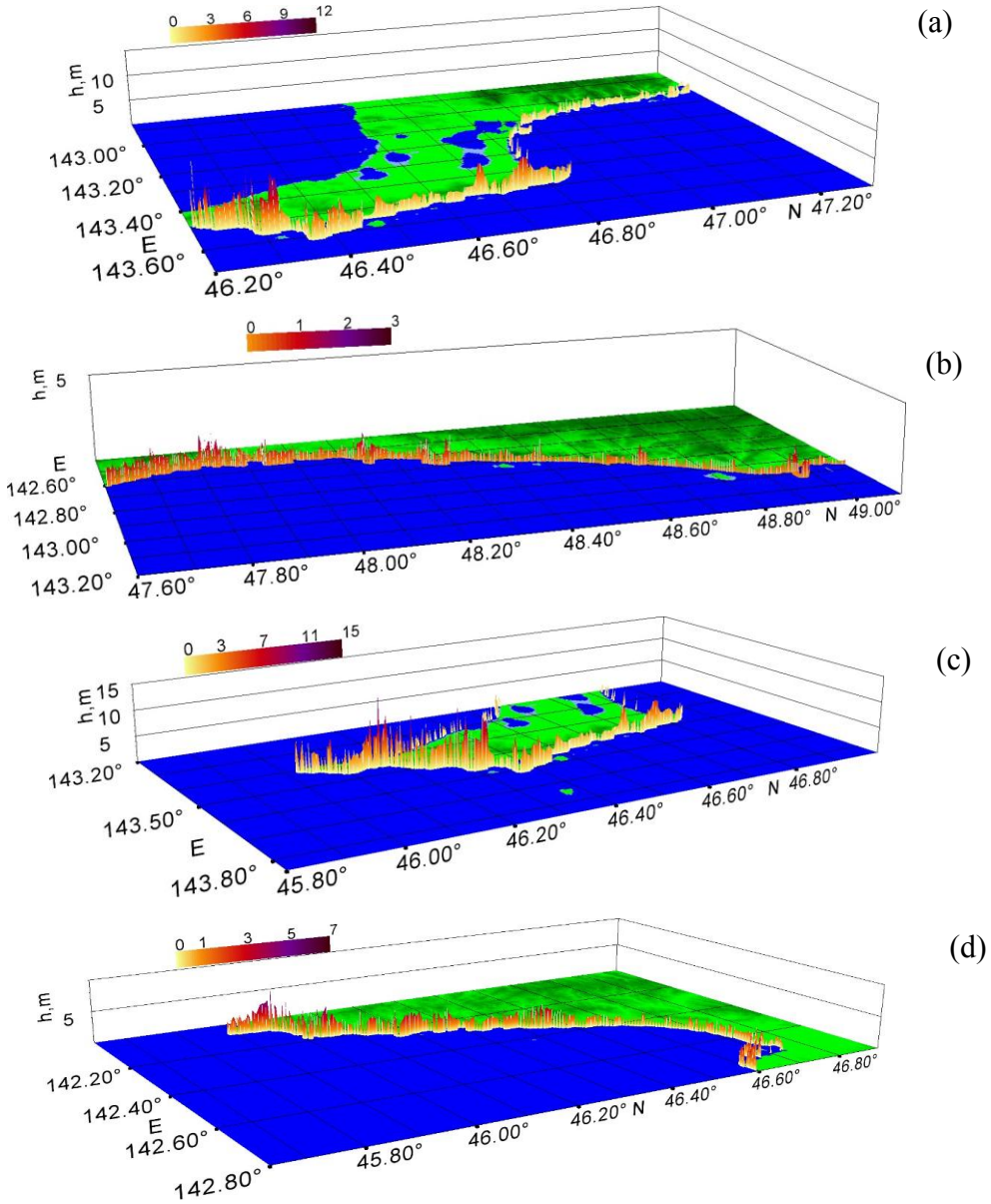

Fig. 17. 3D histograms of maximum wave heights along the coast of Sakhalin during the implementation of the landslide process (Scenario 2): a) a section of the coast near the cities of Dolinsk and Makarov; b) a strip of the coast of the Gulf of Patience; (c) a stretch of coast near Cape Aniva; d) Aniva Bay coast zone, near the town of Korsakov.

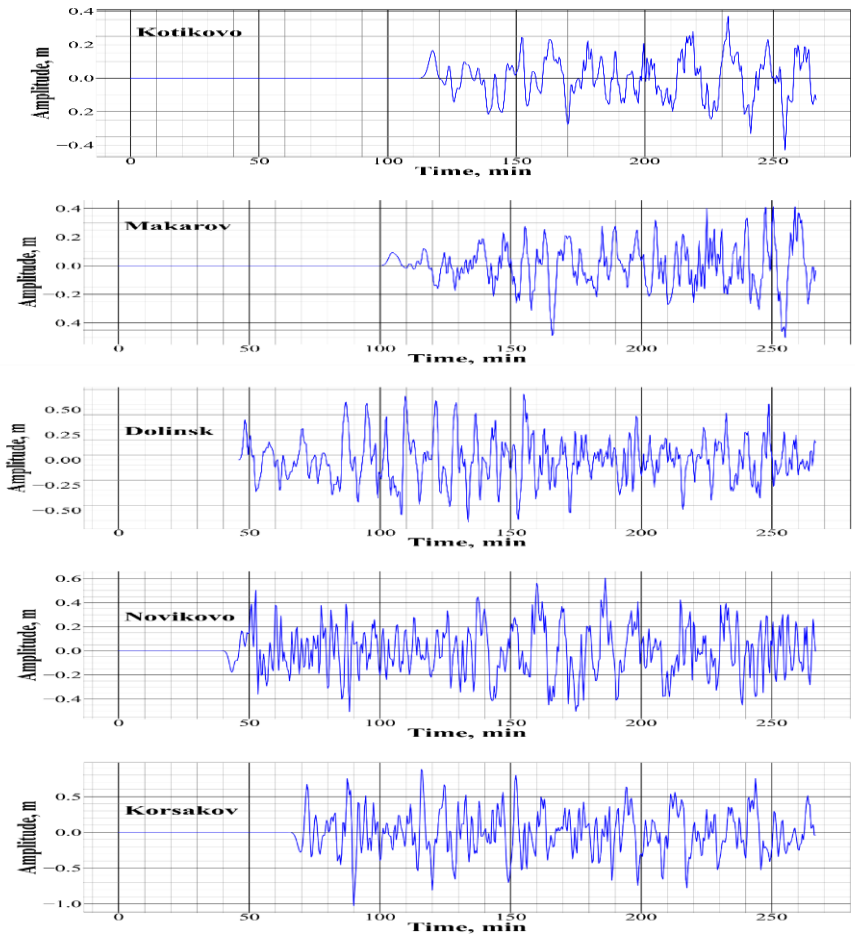

Fig.18. Tide-gauge records of the coast of Aniva Bay (Sakhalin Island, Scenario 2)

According to the data of tide-gauge records, it can be seen that at such points as Kotikovo, Vladimirovo, Poronaysk and Dolinsk, the wave arrived with a positive phase, i.e., the tsunami began with a wave runup onto the shore, in the range from 0.1 to 0.2 meters. In the points of Korsakovo and Novikovo, adjacent to the source, a low tide of up to 0.3 meters is observed, followed by the arrival of a wave up to 0.5 meters high, and this first wave is not the highest at these points. Also, according to the data from tide-gauge records, one can see the spread of wave heights, which is 1.9 m: from + 0.88 to-1.025 meters.

4. CONCLUSIONS

The work considered landslide processes in the Kuril Basin on the western slope in the Sea of Okhotsk. In the computation, data from the work of Baranov V.V. et al. [3] on the western slope of the Kuril Basin in the Sea of Okhotsk were used. The considered landslide processes were modeled on the basis of studies of international marine expeditions of the Russian Academy of Sciences. Four scenarios were considered, two landslide processes, two of which are presented in this article. Two scenarios for localizing a landslide opposite Cape Patience and two scenarios for localizing a landslide opposite Cape Aniva were considered. Landslide processes were modeled within the framework of a solid-block segmental model of a landslide source. During the movement of the landslide, a tsunami source and tsunami wave fronts were generated, the

propagation of which was considered in part of the Sea of Okhotsk, along the. Sakhalin Island. It should be noted that at the points of Cape Aniva and Cape Patience, peaks in wave height are observed, which is possibly associated with resonance phenomena. Compared to the computations in [6], where the landslide process was considered, with the center at the point 51.5°N; 145.4°E, the data differ. For example, in the study [6], the waves that reached the coast of Sakhalin Island in the area of the village of Nogliki had an average height of 3 to 6 meters, moreover. The height peak was reached at the Molikpak platform and was equal to 16 m. In our computations, the average wave heights in this section are from 1 to 3 m, and the peak falls on Cape Patience and reaches 14 m. However, it should be noted that the localization of landslide masses in both cases is significantly different. The landslide in [6] is located to the north of the landslide localized in the Kuril Basin (Scenario 1), which well explains the lower average heights in our computation.

Acknowledgements

The authors acknowledge the funding of this study provided by grant of President of the Russian Federation for the state support of Leading Scientific Schools of the Russian Federation (Grant No. NSH-70.2022.1.5).

REFERENCES

1. Soloviev S.L., Go Ch.N. Catalog of tsunamis on the West Pacific coast. – M.: Nauka, 1974. 310 p.
2. Shchetnikov N.A. Tsunami on the coast of Sakhalin and the Kuril Islands from tide-gauge data 1952-1968. – Vladivostok: Far Eastern Branch of the Academy of Sciences of the USSR, 1990 24 p.
3. Baranov B.V., Prokudin V.G., Dzhin Ya.-K., Dozorova K.A., Rukavishnikova D.D.. Underwater landslides on the western slope of the Kuril Basin of the Sea of Okhotsk // Oceanologia. 2018. V. 58. No. 3. P. 452–462.
4. www. sakhmeteo.ru
5. Zaitsev A.I., Kostenko I.S., Kurkin A.A., Pelinovsky E.N. Tsunami on Sakhalin Island: Observations and Numerical Modeling. - Nizhny Novgorod: Nizhny Novgorod. State Tech. Univ. n.a. R.E. Alekseev, 2016. 122 p.
6. Ivanova A.A., Kulikova E.A., Fine I.V., Baranov B.V.. Generation of a Tsunami from the Submarine Landslide Near the East Coast of Sakhalin Island // Moscow University Physics Bulletin. 2018. V. 73. No. 2. P. 234–239.
7. Lobkovsky L.I., Mazova R.Kh., Kataeva L.Yu., Baranov B.V. Generation and propagation of catastrophic tsunamis in the Sea of Okhotsk. Possible scenarios // Doklady RAS. 2006. V. 410. No. 4. P. 528–531.
8. Schiermeier Q. Huge Landslide triggered rare Greenland mega-tsunami // Nature. 2017. https://doi.org/10.1038/nature..22374
9. Heidarzadeh M., Ishibe T., Sandanbata O., Muhari A., Wijanarto A.B. Numerical modeling of the subaerial landslide source of the 22 December 2018 Anak Krakatoa volcanic tsunami, Indonesia // Ocean Eng. 2020. V. 195. Art. No. 106733.
10. Iwasaki S.-I., Furumoto A., Honza E. Can be a submarine landslide be considered as a tsunami source? // Science of Tsunami Hazards. 1996. V. 14. P. 89-100.
11. Iwasaki S.-I. The wave forms and directivity of a tsunami generated by an earthquake and landslide // Science of Tsunami Hazards. 1997. V. 15. P. 23-40.

12. Pelinovsky E., Poplavsky A. Simplified model of tsunami generation by submarine landslides // Physics and Chemistry of the Earth. 1996. V. 21. P. 13-17.
13. Didenkulova I., Nikolkina I., Pelinovsky E., Zahibo N. Tsunami waves generated by submarine landslides of variable volume: analytical solutions for a basin of variable depth // Nat. Hazards Earth Syst. Sci. 2010. V. 10. No. 11. P. 2407–2419.
14. Jiang L., LeBlond P.H. Numerical modeling of an underwater Bingham plastic mudslide and the waves which it generates // J. Geophys. Res. 1993. V.98. No. C6. P.10.303-10.317.
15. Jiang L., LeBlond P.H. Three-dimensional modeling of tsunami generation due to a submarine mudslide // J. Phys. Oceanogr. 1994. V.24. No. 3. P.559-572
16. Fine I.V., Rabinovich A.B., Thomson R.E., Kulikov E.A. Numerical modeling of tsunami generation by submarine and subaerial landslides // In: Submarine Landslides and Tsunamis (Eds.: A.C. Yalciner, E.N. Pelinovsky, E. Okal, C.E. Synolakis), NATO Science Series, IV. Earth & Environmental Sciences, Kluwer Acad. Publ. 2003. V. 21. P. 69-88.
17. Fine I.V., Rabinovich A.B., Bornhold B.D., Thomson R.E., Kulikov E.A. The Grand Banks landslide-generated tsunami of November 18 1929: preliminary analysis and numerical modeling // Marine Geology. 2005. V. 215. P. 45-57.
18. Ostapenko V.V. Numerical modeling of wave currents caused by a coastal landslide // Appl. Math. 1999. V. 40. No. 4. P. 109–117.
19. Fedotova Z. I., Chubarov L. B., Shokin Yu. I. Simulation of surface waves generated by landslides // Comp. Technology. 2004. V. 9. No. 6. P. 89–96.
20 Marchuk An.G. Numerical modeling of the resonant tsunami generation by the submarine landslide // Bull. Nov. Comp. Center , Math. Model. in Geoph. 2008. V. 12. P. 45–54.
21. Khakimyazov G.S., Shokina N.Yu. Numerical modeling of surface waves arising from the movement of an underwater landslide on an uneven bottom // Comp. Technology. 2010. V. 15. No. 1. P. 105–119.
22. Chernyshov A.D. On the conditions of snow avalanches and ground landslides // Izv. RAS. MTT. 2013. No. 3. P. 135-143.
23. De Blasio F.V., Elverhoi A., Issler D., Harbitz C.B., Bryn P., Lien R. Flow models of natural debris flows originating from overconsolidated clay material // Marine Geol. 2004. V. 213. P. 439-455.
24. Liu W, He S. A two-layer model for simulating landslide dam over mobile river beds // Landslides. 2016. V. 13. P. 565-576.
25 Ma G, Kirby J.T., Shi F. Numerical simulations of tsunami waves generated by deformable submarine landslides // Ocean Modeling. 2013. V. 69. P. 146-165.
26. Garagash I.A., Chemenda A. Numerical modeling of submarine landsliding triggered by seismic and tectonic processes // In: Proc. of 2nd Taiwan-France Symposium on Natural Hazards Mitigation: Methods and Applications, Villfranchesur-Mer (SE France), 2003.
27. Papadopoulos G.A., Lobkovsky L.I., Mazova R.Kh., Garagash I.A., Karastathis V., Kataeva L.Yu., Kaz'min V.G. Numerical Modeling of Sediment Mass Sliding and Tsunami Generation: the Case of 7 February 1963, in Corinth Gulf, Greece // Marine Geodesy. 2007. V. 30. P. 335-344.
28. Lobkovsky L., Mazova R., Remizov I. et al. Local tsunami run-up depending on initial localization of the landslide body at submarine slope // Landslides. 2021. V. 18. P. 897–907.
29. Marchuk A.G., Chubarov L.B., Shokin Yu.I. Numerical modeling of tsunami waves. – Novosibirsk: Nauka, 1983. 160 p.
30. Voltsinger N.E., Klevanny K.A., Pelinovsky E.N. Long-wave dynamics of the coastal zone. – Leningrad: Gidrometeoizdat, 272 p.